
Appendix A. Measurement of short pulse response and frequency response function of non-canonical 3D objects

A.1. Measurement set-up

In order to study experimentally the transient backscattering of 3D objects, a Time Domain Scattering Range (TDSR) has been developed at the RMA [1]. The system consists of the following parts (Fig. 1). On the transmitting side, a 2 meter long monocone antenna on a square ground plane (3 m x 3 m) is coaxially fed by a fast step-function generator. On the receiving side, a broadband electric field sensor, which is connected to a 20 GHz digitising oscilloscope through a set of UWB low noise amplifiers, detects the transient wave. The 3D Device Under Test (DUT) is put on the ground plane and is illuminated by a transient spherical wave, radiated between the monocone and the ground plane. The backscattering on the DUT is measured by the broadband electric field sensor. Because the long monocone antenna radiates a step function and because the electric field sensor is a time derivative sensor, its output yields in fact the impulse response of the device under test.

Three solid state generators are available in the laboratory to feed the antenna. The first two generators generate a repetitive step function (50V/350ps, 10V/45ps) with a high waveform purity. The third generator yields a 2kV/200ps impulse waveform. The fastest generator (10V/45ps) confers to the TDSR a sub-centimetre radial

resolution on the target, which makes it possible to resolve the different scattering centres of the target and to quantify their relative amplitudes. The oscilloscope is coupled to a personal computer for collecting and analysing the data.

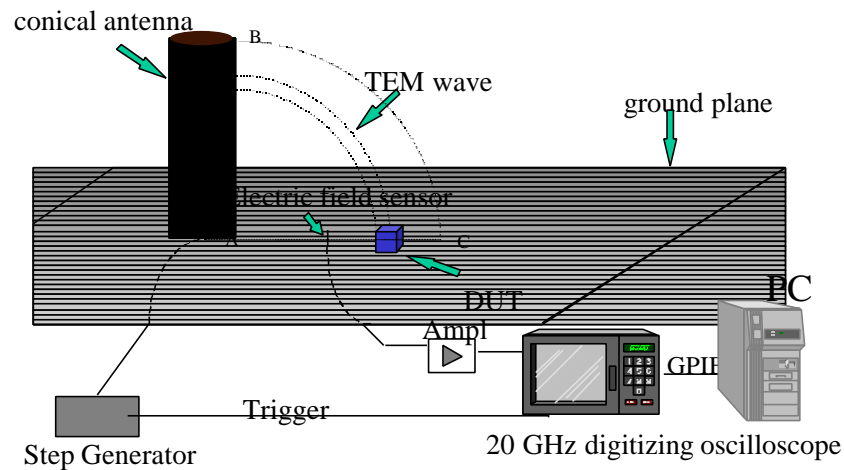


Fig. 1: The Time Domain Scattering Range at the RMA

A.2. Measurement of the FRF of 3D objects by dual channel analysis

The main objective in dual channel systems analysis is to measure input-output relationships of linear systems. In our case the 3D object in free space will be considered as a linear system. Two fundamental functions of this analysis, the Frequency Response Function (FRF) and the Coherence Function, are dealt with in some detail.

Every time-invariant, stable and linear system is completely described in the time domain by its Impulse Response (IR) $h(t)$, which mathematically relates the input $x(t)$ and the output $y(t)$ of the system according to the convolution integral. In the frequency domain this relationship is given by

$$Y(f) = H(f)X(f) \quad (\text{A. 1})$$

where $X(f)$ and $Y(f)$ are the Fourier transform of input $x(t)$ and the output $y(t)$. $H(f)$ is called the Frequency Response Function. $H(f)$ and $h(t)$ are related by the Fourier transform and contain the same information.

Theoretically, the FRF $H(f)$ can be calculated using (A.1) by dividing $Y(f)$ by $X(f)$. In practice this is impossible because (A.1) degrades very fast in the presence of noise. The best way to handle the noise problem is to perform multiple measurements of input and output and estimate the FRF in the least squares sense to obtain the best linear fit in the frequency band covered by the input signal $x(t)$. There exist different FRF estimators [2]. In our application the power of the output signal is far less than the power in the input signal, so the S/N ratio of the output signal will be very low. In this case the best estimator is

$$\tilde{H}_1 = \frac{\sum_{k=1}^K YX^*}{\sum_{k=1}^K XX^*} \quad (\text{A. 2})$$

where $*$ indicates the complex conjugation and K the number of measurements of input and output signal.

Equation (A.2) will minimise uncorrelated measurement noise at the output in a least square sense.

For $K \rightarrow \infty$ equation (A.2) becomes

$$\tilde{H}_1 = \frac{S_{yx}}{S_{xx}} \quad (\text{A. 3})$$

with S_{xx} and S_{yx} the autospectrum and the cross-spectrum of the input and output signals.

Another useful Dual Channel function is the so-called Coherence Function $g^2(f)$, given by

$$g^2(f) = \frac{|S_{xy}|^2}{S_{xx}S_{yy}} \quad \text{with } 0 < g^2(f) < 1 \quad (\text{A. 4})$$

For a given frequency, a low Coherence (< 0.8) will indicate that one or more of the following conditions exist:

- extraneous noise is present in the measurement at that frequency
- the system is not linear
- there are other inputs, besides $x(t)$, influencing the output.

Hence $g^2(f)$ will give an idea of the quality of the measurements and of the assumptions that are made about the system. A coherence $g^2(f) > 0.8$ is needed for an accurate interpretation of the measured data.

The measurement set-up for the dual channel analysis is represented in Fig. 2.

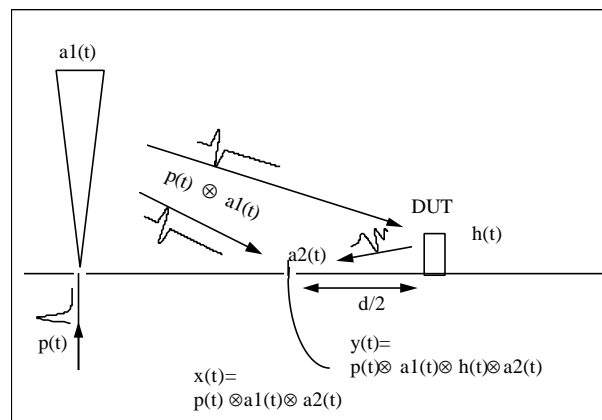


Fig. 2: Measurement set-up for dual channel analysis

Assume the 3D target as a linear system with Impulse Response $h(t)$. Let $a_1(t)$ be the IR of the transmitting antenna, $a_2(t)$ the IR of the electric field sensor, and $p(t)$ the signal generated by the source. Not taking into account the spreading loss in the free space, one can say that

$$\begin{aligned} \frac{Y(f)}{X(f)} &= \frac{P(f)A_1(f)H(f)A_2(f)e^{-jw\frac{d}{c}}}{P(f)A_1(f)A_2(f)} \\ &= H(f)e^{-jw\frac{d}{c}} \end{aligned} \quad (\text{A. 5})$$

with $X(f)$ the Fourier transform of the pulse sent by the monocone and captured by the electric field sensor. $Y(f)$ is the Fourier transform of the signal backscattered by the target, and captured by the electric field sensor, taking into account the delay caused by the travelling time of the signal. d is twice the distance between the target and the electric field sensor. By measuring K times the input $x(t)$ and the output $y(t)$, (A.2) yields an estimation of the FRF $\tilde{H}(f) e^{-jw\frac{d}{c}}$ of the 3D object. The delay $e^{-jw\frac{d}{c}}$, which only influences the phase, is a function of the travelling time and can be calculated.

The advantage of this test set-up is that one can measure the input and the output signals, separated in time by $\frac{d}{c}$, with the same sensor. This means that the measured FRF of the 3D object does not depend on the IR $a_2(t)$ of the electric field sensor. The excitation signal $p(t) \otimes a_1(t)$ is of great importance because the measured FRF is only meaningful at the frequencies excited by this input signal. Since the noise spectral density can be regarded as more or less uniform over the frequency range of interest, the signal to noise ratio will become too small for frequencies with too little power and, as a consequence, the coherence function will be less than 0.8. Fig. 3. shows the coherence function of a typically dual channel measurement performed with the TDSR when the fastest generator (10V/45ps) is used. At frequencies less than 800 MHz or above 13 GHz the coherence function is less than 0.8, meaning that

the TDSR at the RMA can only be used to measure the FRF of 3D objects in that frequency range.

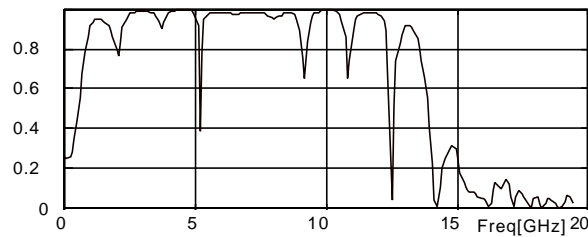


Fig. 3: Coherence function

A.3. Measurement results on Teflon cylinders and AP mines in free space

In a first step, tests are performed on three Teflon cylinders with dimensions comparable to a typical AP mine. The dimensions (in mm) of the cylinders are given in Fig. 4.

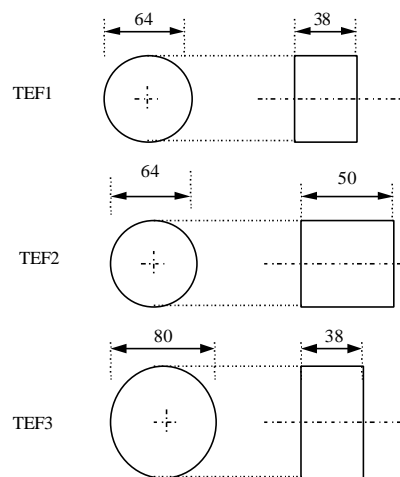


Fig. 4: The three Teflon cylinders

The cylinders are positioned on the ground plane such that the top of the cylinder is oriented towards the transmitting antenna (their surface is perpendicular to the propagation direction of the incoming wave). Fig. 5, Fig. 6 and Fig. 7 show for each

of these cylinders the backscattered signal as a function of time (upper plot) and the magnitude of the FRF as a function of frequency (lower plot). Note that the magnitude of the FRF is not represented in dB's!

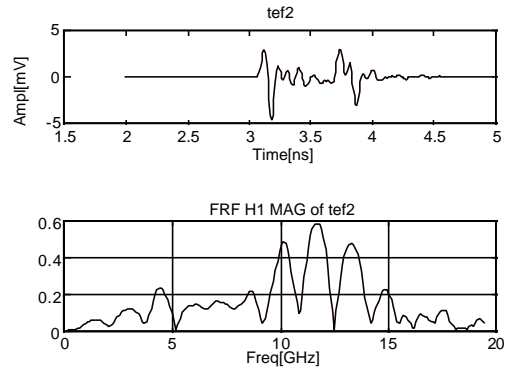
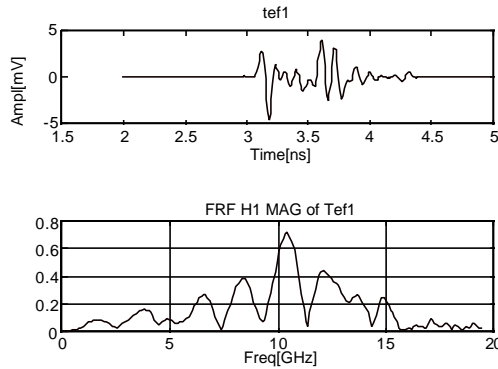


Fig. 5: Short pulse response and FRF of Tef 1 **Fig. 6:** Short pulse response and FRF of Tef 2

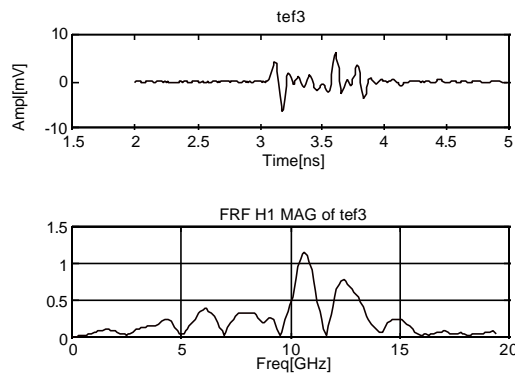


Fig. 7: Short pulse response and FRF of Tef 3

In a second step, tests were performed on two types of AP mines. The first type is the Belgian PRB M35 mine, which is a small AP mine. The dimensions of the PRB M35 are the same as the dimensions of TEF1 (\varnothing 64mm, height 38mm). The TNT of the mine is replaced by a silicone with electrical parameters comparable to those of TNT. The second type of AP mine is a PMN mine (\varnothing 115mm, height 55mm). Fig. 8 and Fig. 9 show for each of these AP mines the backscattered signal as a function of time (upper plot) and the magnitude of the FRF as a function of frequency (lower plot).

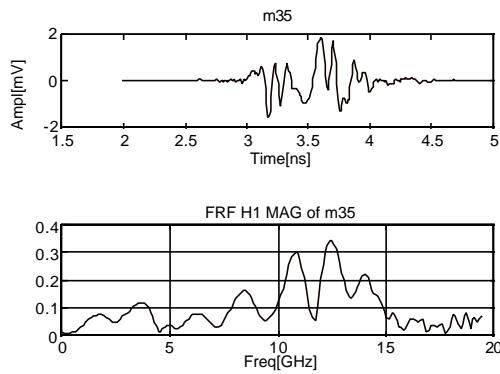


Fig. 8: Short pulse response and FRF of PRB M35

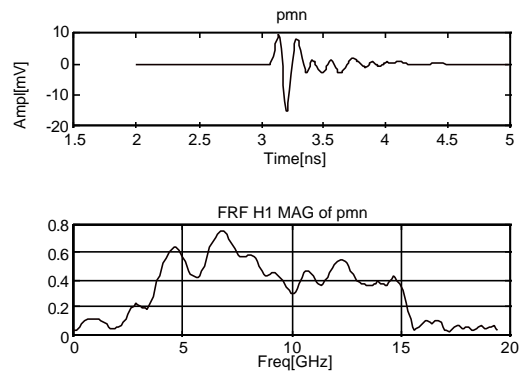


Fig. 9: Short pulse response and FRF of PMN

A.4. Discussion

Tests have been performed on Teflon cylinders and on AP mines in free space. In the backscattered signal of the objects, the scattering centres or the different backscattering mechanisms clearly appear. On the other hand, looking at the magnitude of the FRFs of the different objects, the peaks in the FRF are not sharp. This indicates that the resonances in the late time response of the objects are damped instantaneously in free space.

REFERENCES

- [1] M. Piette, *Banc de mesure en régime transitoire de la signature radar d'objets tridimensionnels*, Doctoral thesis, Université catholique de Louvain and Royal Military Academy, Belgium, Oct. 1995.
- [2] A. Preumont, *Random Vibration and Spectral Analysis*. Brussels: Kluwer Academic, 1999, pp. 135-141.